

Hindawi
International Journal of Mathematics and Mathematical Sciences
Volume 2018, Article ID 1725671, 14 pages
<https://doi.org/10.1155/2018/1725671>



Research Article

A Mathematical Model for Coinfection of Listeriosis and Anthrax Diseases

Shaibu Osman ¹ and Oluwole Daniel Makinde ²

¹Department of Mathematics, Pan African University, Institute for Basic Sciences, Technology and Innovations, Box 62000-00200, Nairobi, Kenya

²Faculty of Military Science, Stellenbosch University, Private Bag X2, Saldanha 7395, South Africa

Correspondence should be addressed to Shaibu Osman; shaibuo@yahoo.com

Received 8 April 2018; Accepted 9 July 2018; Published 2 August 2018

Academic Editor: Ram N. Mohapatra

Copyright © 2018 Shaibu Osman and Oluwole Daniel Makinde. This is an open access article distributed under the Creative Commons Attribution License, which permits unrestricted use, distribution, and reproduction in any medium, provided the original work is properly cited.

Listeriosis and Anthrax are fatal zoonotic diseases caused by *Listeria monocytogene* and *Bacillus Anthracis*, respectively. In this paper, we proposed and analysed a compartmental Listeriosis-Anthrax coinfection model describing the transmission dynamics of Listeriosis and Anthrax epidemic in human population using the stability theory of differential equations. Our model revealed that the disease-free equilibrium of the Anthrax model only is locally stable when the basic reproduction number is less than one. Sensitivity analysis was carried out on the model parameters in order to determine their impact on the disease dynamics. Numerical simulation of the coinfection model was carried out and the results are displayed graphically and discussed. We simulate the Listeriosis-Anthrax coinfection model by varying the human contact rate to see its effects on infected Anthrax population, infected Listeriosis population, and Listeriosis-Anthrax coinfecting population.

1. Introduction

Listeriosis and Anthrax are fatal zoonotic diseases caused by *Listeria monocytogene* and *Bacillus Anthracis*, respectively. Listeriosis in infants can be acquired in two forms. Mothers usually acquire it after eating foods that are contaminated with *Listeria monocytogenes* and can develop sepsis resulting in chorioamnionitis and delivering a septic infant or fetus. Moreover, mothers carrying the pathogens in the gastrointestinal tract can infect the skin and respiratory tract of their babies during childbirth. *Listeria monocytogenes* are among the commonest pathogens responsible for bacterial meningitis among neonates. Responsible factors for the disease include induced immune suppression linked with HIV infection, hemochromatosis hematologic malignancies, cirrhosis, diabetes, and renal failure with hemodialysis [1].

Authors in [2] developed a model for Anthrax transmission but never considered the transmissions in both animal and human populations. Our model is an improvement of the work done by authors in [2, 3]. Both formulated Anthrax models but only concentrated on the disease transmissions

in animals cases only. Anthrax disease is caused by bacteria infections and it affects both humans and animals. Our model is an improvement of the two models as we considered Anthrax as a zoonotic disease and also looked at sensitivity analysis and the effects of the contact rate on the disease transmissions.

Authors in [4] published a paper on the effectiveness of constant and pulse vaccination policies using SIR model. The analysis of their results under constant vaccination showed that the dynamics of the disease model is similar to the dynamics without vaccination [5, 6]. There are some findings on the spread of zoonotic diseases but a number of these researches focused on the effect of vaccination on the spread and transmission of the diseases as in the case of the authors in [7]. Moreover, authors in [8] investigated a disease transmission model by considering the impact of a protective vaccine and came up with the optimal vaccine coverage threshold required for disease eradication. However, authors in [9] employed optimal control to study a nonlinear SIR epidemic model with a vaccination strategy. Several mathematical modeling techniques have been employed to

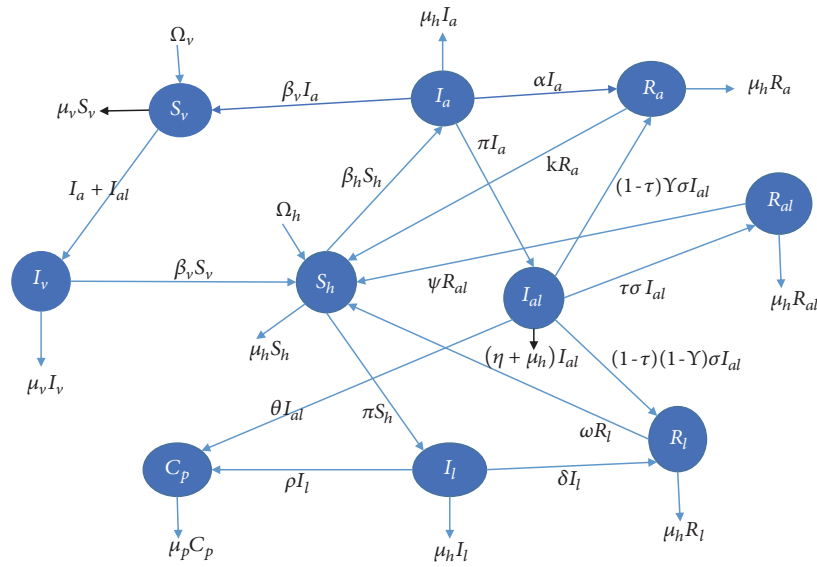


FIGURE 1: Flowchart for the coinfection model.

study the role of optimal control using SIR epidemic model [10–12]. Authors in [13] formulated an SIR epidemic model by considering vaccination as a control measure in their model analysis. Authors in [14] developed a mathematical model for the transmission dynamics of Listeriosis in animal and human populations but did not use optimal control as a control measure in fighting the disease. They divided the animal population into four compartments by introducing the vaccination compartment.

Authors in [15] formulated a model and employed optimal control to investigate the impact of chemotherapy on malaria disease with infection immigrants and [16] applied optimal control methods associated with preventing exogenous reinfection based on an exogenous reinfection tuberculosis model. Authors in [17] conducted a research on the identification and reservoirs of pathogens for effective control of sporadic disease and epidemics. Listeria monocytogenes is among the major zoonotic food borne pathogen that is responsible for approximately twenty-eight percent of most food-related deaths in the United States annually and a major cause of serious product recalls worldwide. The dairy farm has been observed as a potential point and reservoir for Listeria monocytogenes.

Models are widely used in the study of transmission dynamics of infectious diseases. In recent times, the application of mathematical models in the study of infectious diseases has increased tremendously. Hence the emergence of a branch called mathematical epidemiology. Frequent diagnostic tests, the availability of clinical data, and electronic surveillance have facilitated the applications of mathematical models to critical examining of scientific hypotheses and the design of real-life strategies of controlling diseases [18, 19].

Authors in [20] constructed a coinfection model of malaria and cholera diseases with optimal control but never considered sensitivity analysis and analysis of the force of infection. Sensitivity analysis determines the most sensitive parameters to the model and the analysis of the force of

infections determines the effects of the contact rate on the disease transmissions.

2. Model Formulation

In this section, we divide the model into subcompartments (groups) as shown in Figure 1. The total human population (N_h) is divided into subcompartments consisting of susceptible humans (S_h), individuals that are infected with Anthrax (I_a), individuals that are infected with Listeriosis (I_l), individuals that are infected with both Anthrax and Listeriosis (I_{al}), and those that have recovered from Anthrax, Listeriosis, and both Anthrax and Listeriosis, respectively, (R_a), (R_l), and (R_{al}). The total vector population is represented by N_v ; this is divided into subcompartments that consist of susceptible animals (S_v) and animals infected with Anthrax (I_v), where (C_p) is population of carcasses of animals in the soil that may have diet of Anthrax. Carcasses of animals which may have not been properly disposed of have the tendency of generating pathogens. The total vector and human populations are represented as

$$\begin{aligned}
 N_h &= S_h + I_a + I_l + I_{al} + R_a + R_l + R_{al}, \\
 N_v &= S_v + I_v,
 \end{aligned}
 \tag{1}$$

where $\pi = C_p v / (k + C_p)$.

The concentration of carcasses and ingestion rate are denoted as K and v , respectively. Listeriosis related death rates are m and η , respectively, and Anthrax related death rates are ϕ and n , respectively. Waning immunity rates are given by ω , k , and ψ . α , δ , and σ are the recovery rates, respectively, and $\tau(1 - \sigma)$ are the bi-infected persons who have recovered from Anthrax only. The natural death rates of human and vector populations are μ_h and μ_v , respectively, and the modification parameter is given by θ . The coinfecting persons who have

recovered from Listeriosis are denoted by $(1 - \tau)(1 - \sigma)$. This implies that

$$\sigma + \tau(1 - \sigma) + (1 - \tau)(1 - \sigma) = 1. \tag{2}$$

The following differential equations were obtained from the flowchart diagram of the coinfection model in Figure 1:

$$\begin{aligned} \frac{dS_h}{dt} &= \Omega_h + kR_a + \omega R_l + \psi R_{al} - \beta_h I_v S_h - \pi S_h - \mu_h S_h \\ \frac{dI_a}{dt} &= \beta_h I_v S_h - \pi I_a - (\alpha + \mu_h + \phi) I_a \\ \frac{dI_l}{dt} &= \pi S_h - \beta_l I_v I_l - (\delta + \mu_h + m + \rho) I_l \\ \frac{dI_{al}}{dt} &= \beta_h I_v I_l + \pi I_a + (\sigma + \mu_h + \eta + \theta) I_{al} \\ \frac{dR_a}{dt} &= \alpha I_a - (k + \mu_h) R_a + (1 - \tau) \gamma \sigma I_{al} \\ \frac{dR_l}{dt} &= \delta I_l - (\omega + \mu_h) R_l + (1 - \tau)(1 - \gamma) \sigma I_{al} \\ \frac{dR_{al}}{dt} &= \tau \sigma I_{al} - (\psi + \mu_h) R_{al} \\ \frac{dC_p}{dt} &= \rho I_l + \theta I_{al} - \mu_b C_p \\ \frac{dS_v}{dt} &= \Omega_v - \beta_v (I_a + I_{al}) S_v - \mu_v S_v \\ \frac{dI_v}{dt} &= \beta_v (I_a + cI) S_v - \mu_v I_v \end{aligned} \tag{3}$$

3. Analysis of Listeriosis Only Model

In this section, only the Listeriosis model is considered in the analysis of the transmission dynamics.

$$\begin{aligned} \frac{dS_h}{dt} &= \Omega_h + \omega R_l - \pi S_h - \mu_h S_h \\ \frac{dI_l}{dt} &= \pi S_h - (\delta + \mu_h + m) I_l \\ \frac{dR_l}{dt} &= \delta I_l - (\omega + \mu_h) R_l \\ \frac{dC_p}{dt} &= \rho I_l - \mu_b C_p \end{aligned} \tag{4}$$

3.1. Disease-Free Equilibrium. We obtain the disease-free equilibrium of the Listeriosis only model by setting the system of equations in (4) to zero. At disease-free equilibrium, there are no infections and recovery.

$$\begin{aligned} \Omega_h + \omega R_l - \pi S_h - \mu_h S_h &= 0 \\ S_h &= \frac{\Omega_h}{\mu_h} \\ \xi_{0l} &= (S_h^*, I_l^*, R_l^*, C_p^*) = \left(\frac{\Omega_h}{\mu_h}, 0, 0, 0 \right). \end{aligned} \tag{5}$$

3.2. Basic Reproduction Number. In this section, the concept of the Next-Generation Matrix would be employed in computing the basic reproduction number. Using the theorem in Van den Driessche and Watmough [21] on the Listeriosis model in (4), the basic reproduction number of the Listeriosis only model, (\mathfrak{R}_{0l}) , is given by

$$\mathfrak{R}_{0l} = \frac{\nu \rho \Omega_h}{\mu_b \mu_h K (\delta + \mu_h + m)} \tag{6}$$

3.3. Existence of the Disease-Free Equilibrium

3.4. Endemic Equilibrium. The endemic equilibrium points are computed by setting the system of differential equations in the Listeriosis only model (4) to zero. The endemic equilibrium points are as follows:

$$\begin{aligned} S_h^* &= \frac{\Omega_h + \omega R_l^*}{\mu_h + \pi^*}, \\ I_l^* &= \frac{\pi^* S_h^*}{(\delta + \mu_h + m)}, \\ R_l^* &= \frac{\delta I_l^*}{\omega + \mu_h}, \\ C_p^* &= \frac{\rho I_l^*}{\mu_b}. \\ \xi_{0l} &= (S_h^*, I_l^*, R_l^*, C_p^*) \\ &= \left(\frac{\Omega_h + \omega R_l^*}{\mu_h + \pi^*}, \frac{\pi^* S_h^*}{(\delta + \mu_h + m)}, \frac{\delta I_l^*}{\omega + \mu_h}, \frac{\rho I_l^*}{\mu_b} \right). \end{aligned} \tag{7}$$

$$\begin{aligned} S_h^* &= \frac{\Omega_h + \omega R_l^*}{\mu_h + \pi^*} \\ I_l^* &= \frac{\pi^* S_h^*}{(\delta + \mu_h + m)} \\ R_l^* &= \frac{\delta I_l^*}{\omega + \mu_h} \\ C_p^* &= \frac{\rho I_l^*}{\mu_b} \end{aligned} \tag{8}$$

3.5. Existence of the Endemic Equilibrium

Lemma 1. *The Listeriosis only model has a unique endemic equilibrium if and only if the basic reproduction number $\mathfrak{R}_{0l} > 1$.*

Proof. The Listeriosis force of infection, $(\pi = C_p \nu / (K + C_p))$, satisfies the polynomial;

$$P(\pi^*) = A(\pi^*)^2 + B(\pi^*) = 0 \tag{9}$$

where $A = \Omega_h \rho (\omega + \mu_h) + \mu_b K (m(\omega + \mu_h) + \mu_h (\delta + \mu_h + \omega))$, and

$$B = (\omega + \mu_h) (1 - R_{0l}). \tag{10}$$

By mathematical induction, $A > 0$ and $B > 0$ whenever the basic reproduction number is less than one ($\mathfrak{R}_{0l} < 1$). This implies that $\pi^* = -B/A \leq 0$. In conclusion, the Listeriosis model has no endemic equilibrium and the basic reproductive number is less than one ($\mathfrak{R}_{0l} < 1$). \square

The analysis illustrates the impossibility of backward bifurcation in the Listeriosis model, because there is no existence of endemic equilibrium whenever the basic reproduction number is less than one ($\mathfrak{R}_{0l} < 1$).

4. Analysis of Anthrax Only Model

In this section, only the Anthrax model is considered in the analysis of the transmission dynamics.

$$\begin{aligned} \frac{dS_h}{dt} &= \Omega_h + kR_a - \beta_h I_v S_h - \mu_h S_h \\ \frac{dI_a}{dt} &= \beta I_v S_h - (\alpha + \mu_h + \phi) I_a \\ \frac{dR_a}{dt} &= \alpha I_a - (k + \mu_h) R_a \\ \frac{dS_v}{dt} &= \Omega_v - \beta_v I_a S_v - \mu_v S_v \\ \frac{dI_v}{dt} &= \beta_v I_a S_v - \mu_v I_v \end{aligned} \quad (11)$$

4.1. Disease-Free Equilibrium. The disease-free equilibrium of the Anthrax only model is obtained by setting the system of equations in model (11) to zero. At disease-free equilibrium, there are no infections and recovery.

$$\begin{aligned} \Omega_h + kR_a - \beta_h I_v S_h - \mu_h S_h &= 0 \\ S_h &= \frac{\Omega_h}{\mu_h} \\ \Omega_v - \beta_v I_a S_v - \mu_v S_v &= 0 \\ S_v &= \frac{\Omega_v}{\mu_v} \\ \xi_{0a} = (S_h^*, I_a^*, R_a^*, S_v^*, I_v^*) &= \left(\frac{\Omega_h}{\mu_h}, 0, 0, \frac{\Omega_v}{\mu_v}, 0 \right). \end{aligned} \quad (12)$$

4.2. Basic Reproduction Number. In this section, the concept of the Next-Generation Matrix would be employed in computing the basic reproduction number. Using the theorem in Van den Driessche and Watmough [21] on the Anthrax model in (11), the basic reproduction number of the Anthrax only model, (\mathfrak{R}_{0a}), is given by

$$\mathfrak{R}_{0a} = \sqrt{\frac{\Omega_h \Omega_v \beta_h \beta_v}{\mu_h \mu_v^2 (\alpha + \mu_h + \phi)}} \quad (14)$$

4.3. Stability of the Disease-Free Equilibrium. Using the next-generation operator concept in Van den Driessche and

Watmough [21] on the systems of equations in model (11), the linear stability of the disease-free equilibrium, (ξ_{0a}), can be ascertained. The disease-free equilibrium is locally asymptotically stable whenever the basic reproduction number is less than one ($\mathfrak{R}_{0a} < 1$). And it is unstable whenever the basic reproduction number is greater than one ($\mathfrak{R}_{0a} > 1$). The disease-free equilibrium is the state at which there are no infections in the system. At disease-free equilibrium, there are no infections in the system.

4.4. Endemic Equilibrium. The endemic equilibrium points are computed by setting the system of differential equations in the Anthrax only model (11) to zero. The endemic equilibrium points are as follows:

$$\begin{aligned} S_h &= \frac{\Omega_h + kR_a^*}{\mu_h + \beta_h I_v^*}, \\ I_a^* &= \frac{\beta_v S_h^* I_v^*}{(\alpha + \mu_h + \phi)}, \\ R_a^* &= \frac{\alpha I_a^*}{k + \mu_h}, \\ S_v^* &= \frac{\Omega_v}{\mu_v + \beta_v I_a^*}, \\ I_v^* &= \frac{\beta_v S_v^* I_a^*}{\mu_v}. \end{aligned} \quad (15)$$

The endemic equilibrium of the Anthrax only model is given by

$$\xi_{0a} = (S_h^*, I_a^*, R_a^*, S_v^*, I_v^*) = \left(\frac{\Omega_h + kR_a^*}{\mu_h + \beta_h I_v^*}, \frac{\beta_v S_h^* I_v^*}{(\alpha + \mu_h + \phi)}, \frac{\alpha I_a^*}{k + \mu_h}, \frac{\Omega_v}{\mu_v + \beta_v I_a^*}, \frac{\beta_v S_v^* I_a^*}{\mu_v} \right) \quad (16)$$

$$\xi_{0a} = \left(\frac{\Omega_h + kR_a^*}{\mu_h + \beta_h I_v^*}, \frac{\beta_v S_h^* I_v^*}{(\alpha + \mu_h + \phi)}, \frac{\alpha I_a^*}{k + \mu_h}, \frac{\Omega_v}{\mu_v + \beta_v I_a^*}, \frac{\beta_v S_v^* I_a^*}{\mu_v} \right) \quad (17)$$

4.5. Existence of the Endemic Equilibrium

Lemma 2. *The Anthrax only model has a unique endemic equilibrium whenever the basic reproduction number (\mathfrak{R}_{0a}) is greater than one ($\mathfrak{R}_{0a} > 1$).*

Proof. Considering the endemic equilibrium points of the Anthrax only model,

$$\xi_{0a} = \left(\frac{\Omega_h + kR_a^*}{\mu_h + \beta_h I_v^*}, \frac{\beta_v S_h^* I_v^*}{(\alpha + \mu_h + \phi)}, \frac{\alpha I_a^*}{k + \mu_h}, \frac{\Omega_v}{\mu_v + \beta_v I_a^*}, \frac{\beta_v S_v^* I_a^*}{\mu_v} \right). \quad (18)$$

The endemic equilibrium point satisfies the given polynomial

$$P(I_a^*) = A_1 (I_a^*)^2 + B_1 (I_a^*) = 0 \tag{19}$$

where

$$A_1 = \beta_v (\Omega_v \beta_h (k\phi + \mu_h (\alpha + k + \phi + \mu_h)) + \mu_h (k + \mu_h) (\alpha + \phi + \mu_h) \mu_v) \tag{20}$$

and

$$B_1 = (k + \mu_h) (1 - R_{0a}^2). \tag{21}$$

By mathematical induction, $A_1 > 0$ and $B_1 > 0$ whenever the basic reproduction number is less than one ($\mathfrak{R}_{0a} < 1$). This implies that $I_a^* = -B_1/A_1 \leq 0$. In conclusion, the Anthrax only model has no endemic any time the basic reproductive number is less than one ($\mathfrak{R}_{0a} < 1$). \square

The analysis illustrates the impossibility of backward bifurcation in the Anthrax only model. Because there is no existence of endemic equilibrium whenever the basic reproduction number is less than one ($\mathfrak{R}_{0a} < 1$).

5. Anthrax-Listeriosis Coinfection Model

In this section, the dynamics of the Anthrax-Listeriosis coinfection model in (3) is considered in the analysis of the transmission dynamics.

5.1. Disease-Free Equilibrium. The disease-free equilibrium of the Anthrax-Listeriosis model is obtained by setting the system of equations of model (3) to zero. At disease-free equilibrium, there are no infections and recovery.

$$\begin{aligned} \Omega_h + kR_a + \omega R_l + \psi R_{al} - \beta_h I_v S_h - \pi S_h - \mu_h S_h &= 0 \\ S_h &= \frac{\Omega_h}{\mu_h} \\ \Omega_v - \beta_v (I_a + cI_{al}) S_v - \mu_v S_v &= 0 \\ S_v &= \frac{\Omega_v}{\mu_v} \end{aligned} \tag{22}$$

The disease-free equilibrium is given by

$$\xi_{0al} = (S_h^*, I_l^*, I_a^*, I_{al}^*, R_l^*, R_a^*, R_{al}^*, C_p^*, S_v^*, I_v^*) \tag{23}$$

$$\xi_{0al} = \left(\frac{\Omega_h}{\mu_h}, 0, 0, 0, 0, 0, 0, \frac{\Omega_v}{\mu_v}, 0 \right) \tag{24}$$

5.2. Basic Reproduction Number. The concept of the next-generation operator method in Van den Driessche and Watmough [21] was employed on the system of differential equations in model (3) to compute the basic reproduction number of the Anthrax-Listeriosis coinfection model. The Anthrax-Listeriosis coinfection model has a reproduction number (\mathfrak{R}_{al}) given by

$$\mathfrak{R}_{al} = \max \{ \mathfrak{R}_a, \mathfrak{R}_l \} \tag{25}$$

where \mathfrak{R}_a and \mathfrak{R}_l are the basic reproduction numbers of Anthrax and Listeriosis, respectively.

$$\mathfrak{R}_a = \sqrt{\frac{\Omega_h \Omega_v \beta_h \beta_v}{\mu_h \mu_v^2 (\alpha + \mu_h + \phi)}} \tag{26}$$

and

$$\mathfrak{R}_l = \frac{\nu \rho \Omega_h}{\mu_b \mu_h K} \left(\frac{(\sigma + \mu_h + \eta + \theta) + \theta (\delta + \mu_h + m)}{(\delta + \mu_h + m) (\sigma + \mu_h + \eta + \theta)} \right) \tag{27}$$

Theorem 3. *The disease-free equilibrium (ξ_{0al}) is locally asymptotically stable whenever the basic reproduction number is less than one ($\mathfrak{R}_{al} < 1$) and unstable otherwise.*

5.3. Impact of Listeriosis on Anthrax. In this section, the impact of Listeriosis on Anthrax and vice versa is analysed. This is done by expressing the reproduction number of one in terms of the other by expressing the basic reproduction number of Listeriosis on Anthrax, that is, expressing \mathfrak{R}_l in terms of \mathfrak{R}_a

$$\text{from } \mathfrak{R}_a = \sqrt{\Omega_h \Omega_v \beta_h \beta_v / \mu_h \mu_v^2 (\alpha + \mu_h + \phi)}.$$

Solving for μ_h in the above,

$$\mu_h = \frac{-G_1 \mathfrak{R}_a + \sqrt{G_1^2 \mathfrak{R}_a^2 + 4G_2}}{2\mu_v \mathfrak{R}_a}, \tag{28}$$

where

$$G_1 = \mu_v (\alpha + \phi) \tag{29}$$

$$\text{and } G_2 = \Omega_h \Omega_v \beta_h \beta_v$$

Also, letting

$$\sqrt{G_1^2 \mathfrak{R}_a^2 + 4G_2} = G_3 \mathfrak{R}_a + G_4, \tag{30}$$

this implies

$$\mu_h = \frac{\mathfrak{R}_a (G_3 - G_1) + G_4}{2\mu_v \mathfrak{R}_a} \tag{31}$$

By substituting μ_h into the basic reproduction number of Listeriosis (\mathfrak{R}_l),

$$\mathfrak{R}_l = \frac{\mathfrak{R}_{0l} (G_4 + (G_3 - G_1) \mathfrak{R}_a + 2(\sigma + \eta + \theta) \mu_v \mathfrak{R}_a + \theta (G_4 + (G_3 - G_1) \mathfrak{R}_a + 2(m + \delta) \mu_v \mathfrak{R}_a))}{G_4 + (G_3 - G_1) \mathfrak{R}_a + 2(\sigma + \eta + \theta) \mu_v \mathfrak{R}_a} \tag{32}$$

where the basic reproduction number of Listeriosis only model (R_{0l}) is given in the relation

$$\mathfrak{R}_{0l} = \frac{\nu\rho\Omega_h}{\mu_b\mu_hK(\delta + \mu_h + m)}. \tag{33}$$

Now, taking the partial derivative of \mathfrak{R}_l with respect to \mathfrak{R}_a in (32) gives

$$\frac{\partial\mathfrak{R}_l}{\partial\mathfrak{R}_a} = \frac{2G_4\theta(m + \delta - (\sigma + \eta + \theta))\mu_v\mathfrak{R}_{0l}}{[G_4 + (G_3 - G_1 + 2(\sigma + \eta + \theta)\mu_v\mathfrak{R}_a)]^2}. \tag{34}$$

If $(m + \delta) \geq (\sigma + \eta + \theta)$, the derivative $(\partial\mathfrak{R}_l/\partial\mathfrak{R}_a)$, is strictly positive. Two scenarios can be deduced from the derivative $(\partial\mathfrak{R}_l/\partial\mathfrak{R}_a)$, depending on the values of the parameters:

$$\begin{aligned} \frac{\partial\mathfrak{R}_l}{\partial\mathfrak{R}_a} &= 0, \\ \text{and } \frac{\partial\mathfrak{R}_l}{\partial\mathfrak{R}_a} &\geq 0. \end{aligned} \tag{35}$$

- (1) If $\partial\mathfrak{R}_l/\partial\mathfrak{R}_a = 0$, it implies that $(m+\delta) = (\sigma+\eta+\theta)$ and the epidemiological implication is that Anthrax has no significance effect on the transmission dynamics of Listeriosis.
- (2) If $\partial\mathfrak{R}_l/\partial\mathfrak{R}_a > 0$, it implies that $(m+\delta) \geq (\sigma+\eta+\theta)$, and the epidemiological implication is that an increase in Anthrax cases would result in an increase Listeriosis

cases in the environment. That is Anthrax enhances Listeriosis infections in the environment.

However, by expressing the basic reproduction number of Anthrax on Listeriosis, that is expressing \mathfrak{R}_a in terms of \mathfrak{R}_l ,

$$\mu_h = \frac{H_1 - H_2\mathfrak{R}_l + \sqrt{H_3\mathfrak{R}_l^2 + H_4\mathfrak{R}_l + H_5}}{2\mathfrak{R}_l}, \tag{36}$$

where

$$\begin{aligned} H_1 &= (1 + \theta)\mathfrak{R}_{0l}, \\ H_2 &= (m + \delta + \sigma + \eta + \theta) \\ H_3 &= (\sigma + \eta + \theta - m - \delta), \\ H_4 &= 2(\theta - 1)(m + \delta - \sigma - \eta - \theta)\mathfrak{R}_{0l} \\ H_5 &= (1 + \theta)^2\mathfrak{R}_{0l}^2. \end{aligned} \tag{37}$$

By letting

$$\sqrt{H_3\mathfrak{R}_l^2 + H_4\mathfrak{R}_l + H_5} = H_6\mathfrak{R}_l + H_7, \tag{38}$$

it implies that

$$\mu_h = \frac{(H_6 - H_2)\mathfrak{R}_l + H_7 + H_1}{2\mathfrak{R}_l}. \tag{39}$$

Therefore,

$$\mathfrak{R}_a^2 = \frac{4\Omega_h\Omega_v\beta_h\beta_v\mathfrak{R}_l^2}{[(H_6 - H_2)\mathfrak{R}_l + H_7 + H_1][H_7 + H_1 + 2(\alpha + \phi)\mathfrak{R}_l + (H_6 - H_2)\mathfrak{R}_l]\mu_v} \tag{40}$$

Now, taking the partial derivative of \mathfrak{R}_a with respect to \mathfrak{R}_l in equation (40) gives

$$\frac{\partial\mathfrak{R}_a}{\partial\mathfrak{R}_l} = \frac{4(H_7 + H_1)[H_7 + H_1 + (\alpha + \phi + H_6 - H_2)\mathfrak{R}_l]\Omega_h\Omega_v\beta_h\beta_v\mathfrak{R}_l}{[(H_6 - H_2)\mathfrak{R}_l + H_7 + H_1]^2[H_7 + H_1 + (2(\alpha + \phi) + H_6 - H_2)\mathfrak{R}_l]^2\mu_v} \tag{41}$$

If the partial derivative of \mathfrak{R}_a with respect to \mathfrak{R}_l is greater than zero, $(\partial\mathfrak{R}_a/\partial\mathfrak{R}_l > 0)$, the biological implication is that an increase in the number of cases of Listeriosis would result in an increase in the number of cases of Anthrax in the environment. Moreover, the impact of Anthrax treatment on Listeriosis can also be analysed by taking the partial derivative of \mathfrak{R}_a with respect to α , $(\partial\mathfrak{R}_a/\partial\alpha)$.

$$\frac{\partial\mathfrak{R}_a}{\partial\alpha} = -\frac{\alpha}{\alpha + \phi + \mu_h}. \tag{42}$$

Clearly, \mathfrak{R}_a is a decreasing function of α ; the epidemiological implication is that the treatment of Listeriosis would have an impact on the transmission dynamics of Anthrax.

5.4. Analysis of Backward Bifurcation. In this section, the phenomenon of backward bifurcation is carried out by employing the center manifold theory on the system of differential equations in model (3). Bifurcation analysis was carried out by employing the center manifold theory in Castillo-Chavez and Song [22]. Considering the human transmission rate (β_h) and ν as the bifurcation parameters, it implies that $\mathfrak{R}_a = 1$ and $\mathfrak{R}_l = 1$ if and only if

$$\beta_h = \beta_h^* = \frac{\mu_h\mu_v^2(\alpha + \phi + \mu_h)}{\Omega_h\Omega_v\beta_v}, \tag{43}$$

and

$$v = v^* = \frac{\mu_b \mu_h K (\delta + \mu_h + m) (\sigma + \mu_h + \eta + \theta)}{\rho \Omega_h (\sigma + \mu_h + \eta + \theta + \theta (m + \delta + \mu_h))}. \quad (44)$$

By considering the following change of variables,

$$\begin{aligned} S_h &= x_1, \\ I_a &= x_2, \\ I_l &= x_3, \\ I_{al} &= x_4, \\ R_a &= x_5, \\ R_l &= x_6, \\ R_{al} &= x_7, \\ C_p &= x_8, \\ S_v &= x_9, \\ I_v &= x_{10}. \end{aligned} \quad (45)$$

This would give the total population as

$$N = x_1 + x_2 + x_3 + x_4 + x_5 + x_6 + x_7 + x_8 + x_9 + x_{10}. \quad (46)$$

By applying vector notation

$$X = (x_1, x_2, x_3, x_4, x_5, x_6, x_7, x_8, x_9, x_{10})^T. \quad (47)$$

The Anthrax-Listeriosis coinfection model can be expressed as

$$\frac{dX}{dt} = F(X), \quad (48)$$

$$\text{where } F = (f_1, f_2, f_3, f_4, f_5, f_6, f_7, f_8, f_9, f_{10})^T.$$

The following system of differential equations is obtained:

$$\begin{aligned} \frac{dx_1}{dt} &= \Omega_h + kx_5 + \omega x_6 + \psi x_7 - \beta_h x_{10} x_1 - \pi x_1 - \mu_h x_1 \\ \frac{dx_2}{dt} &= \beta_h x_{10} x_1 - \pi x_2 - (\alpha + \mu_h + \phi) x_2 \\ \frac{dx_3}{dt} &= \pi x_1 - \beta_l x_{10} x_3 - (\delta + \mu_h + m + \rho) x_3 \\ \frac{dx_4}{dt} &= \beta_l x_{10} x_3 + \pi x_2 + (\sigma + \mu_h + \eta + \theta) x_4 \end{aligned}$$

$$\frac{dx_5}{dt} = \alpha x_2 - (k + \mu_h) x_5 + (1 - \tau) \gamma \sigma x_4$$

$$\frac{dx_6}{dt} = \delta x_3 - (\omega + \mu_h) x_6 + (1 - \tau) (1 - \gamma) \sigma x_4$$

$$\frac{dx_7}{dt} = \tau \sigma x_4 - (\psi + \mu_h) x_7$$

$$\frac{dx_8}{dt} = \rho x_3 + \theta x_4 - \mu_b x_8$$

$$\frac{dx_9}{dt} = \Omega_v - \beta_v (x_2 + x_4) x_9 - \mu_v x_9$$

$$\frac{dx_{10}}{dt} = \beta_v (x_2 + x_4) x_9 - \mu_v x_{10}$$

(49)

Backward bifurcation is carried out by employing the center manifold theory on the system of differential equations in model (3). This concept involves the computation of the Jacobian of the system of differential equations in (49) at the disease-free equilibrium (ξ_0) . The Jacobian matrix at disease-free equilibrium is given by

$$J(\xi_0) = \begin{bmatrix} -\mu_h & 0 & 0 & J_1 & k & \omega & \psi & J_2 & 0 & J_3 \\ 0 & -J_4 & 0 & 0 & 0 & 0 & 0 & 0 & 0 & J_3 \\ 0 & 0 & -J_5 & J_1 & 0 & 0 & 0 & J_2 & 0 & 0 \\ 0 & 0 & 0 & -J_6 & 0 & 0 & 0 & 0 & 0 & 0 \\ 0 & \alpha & 0 & J_7 & -J_8 & 0 & 0 & 0 & 0 & 0 \\ 0 & 0 & \delta & J_9 & 0 & -J_{10} & 0 & 0 & 0 & 0 \\ 0 & 0 & 0 & \sigma & 0 & 0 & -J_{11} & 0 & 0 & 0 \\ 0 & 0 & \rho & \theta & 0 & 0 & 0 & -\mu_b & 0 & 0 \\ 0 & -J_{12} & 0 & -J_{12} & 0 & 0 & 0 & 0 & -\mu_v & 0 \\ 0 & J_{12} & 0 & J_{12} & 0 & 0 & 0 & 0 & 0 & -\mu_v \end{bmatrix} \quad (50)$$

where

$$J_1 = \frac{\rho \Omega_h}{\mu_h},$$

$$J_2 = \frac{\mu_b (\delta + \mu_h + m) (\sigma + \mu_h + \eta + \theta)}{\rho (\sigma + \mu_h + \eta + \theta + \theta (\delta + \mu_h + m))},$$

$$J_3 = \frac{\mu_v^3 (\alpha + \phi + \mu_h)}{\Omega_v \beta_v},$$

$$J_4 = (\alpha + \phi + \mu_h),$$

$$J_5 = (\delta + \mu_h + m),$$

$$J_6 = (\sigma + \mu_h + \eta + \theta),$$

$$J_7 = (1 - \tau) \gamma \sigma,$$

$$J_8 = (k + \mu_h),$$

$$\begin{aligned}
 J_9 &= (1 - \tau)(1 - \gamma)\sigma, \\
 J_{10} &= (\omega + \mu_h), \\
 J_{11} &= (\psi + \mu_h) \\
 \text{and } J_{12} &= \frac{\Omega_v \beta_v}{\mu_v}.
 \end{aligned}
 \tag{51}$$

Clearly, the Jacobian matrix at disease-free equilibrium has a case of simple zero eigenvalue as well as other eigenvalues with negative real parts. This is an indication that the center manifold theorem is applicable. By applying the center manifold theorem in Castillo-Chavez and Song [22], the left and right eigenvectors of the Jacobian matrix $J(\xi_0)$ are computed first. Letting the left and right eigenvector represented by

$$y = [y_1, y_2, y_3, y_4, y_5, y_6, y_7, y_8, y_9, y_{10}]
 \tag{52}$$

$$\text{and } w = [w_1, w_2, w_3, w_4, w_5, w_6, w_7, w_8, w_9, w_{10}]^T,$$

respectively, the following were obtained:

$$\begin{aligned}
 w_1 &= \frac{Kw_5}{\mu_h} + \frac{w_2\mu_v^2(\alpha + \phi + \mu_h)}{\mu_h}, \\
 w_2 &= \frac{\mu_v^2}{\Omega_v\beta_v}, \\
 w_3 &= w_4 = w_6 = w_7 = w_8 = 0, \\
 w_5 &= \frac{\alpha\mu_v^2}{\Omega_v\beta_v(k + \mu_h)}, \\
 w_9 &= -w_{10}, \\
 w_{10} &= 1.
 \end{aligned}
 \tag{53}$$

And

$$\begin{aligned}
 y_1 &= y_3 = y_5 = y_6 = y_7 = y_8 = y_9 = 0, \\
 y_2 &= \frac{v_{10}\Omega_v\beta_v}{\mu_v(\alpha + \phi + \mu_h)}, \\
 y_2 &= y_4, \\
 y_{10} &= \frac{-\mu_v(\sigma + \mu_h + \eta + \theta)}{\Omega_v\beta_v}.
 \end{aligned}
 \tag{54}$$

Moreover, by further simplifications, it can be shown that

$$\begin{aligned}
 a &= \frac{\tau w_{10} \mu_v^3 (\sigma + \mu_h + \eta + \theta)}{\Omega_v \beta_v} \\
 &\quad - 2w_{10} \beta_v \left[\frac{\mu_v^2 (\sigma + \mu_h + \eta + \theta)}{\mu_h \Omega_v \beta_v} \right. \\
 &\quad \left. + \frac{\alpha K \mu_v^2 (\sigma + \mu_h + \eta + \theta)}{\mu_h \Omega_v \beta_v (k + \mu_h) (\alpha + \phi + \mu_h)} \right], \\
 b &= y_2 w_{10} \frac{\Omega_h}{\mu_h} > 0.
 \end{aligned}
 \tag{55}$$

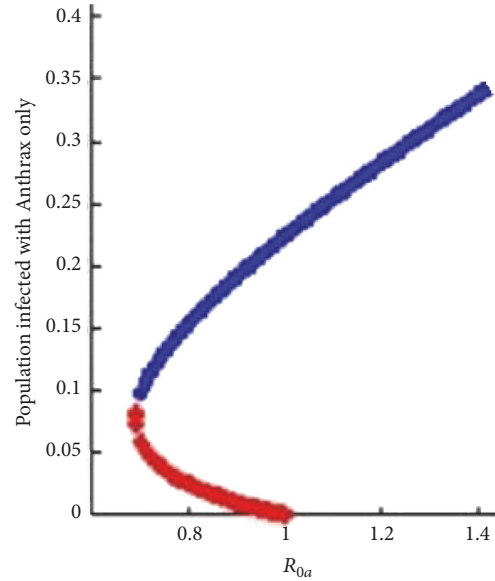


FIGURE 2: Simulation of the coinfection model showing the existence of backward bifurcation.

It can be deduced that the coefficient b would always be positive. Backward bifurcation will take place in the system of differential equations in (3) if the coefficient a is positive. In conclusion, it implies that the disease-free equilibrium is not globally stable.

Figure 2 shows the simulation of the coinfection model indicating the phenomenon of backward bifurcation as evidence to the model analysis. This phenomenon usually exists in cases where the disease-free equilibrium and the endemic equilibrium coexist. Epidemically, the implication is that the concept of whenever the basic reproduction number is less than unity, the ability to control the disease is no longer sufficient. Figure 2 confirms the analytical results which shows that endemic equilibrium exists when the basic reproduction number is greater than unity.

6. Sensitivity Analysis of the Coinfection Model

In this section, we performed the sensitivity analysis of the basic reproduction number of the coinfection model to each of the parameter values. This is to determine the significance or contribution of each parameter on the basic reproduction number. The sensitivity index of the basic reproduction number (\mathfrak{R}_0) to a parameter P is given by the relation

$$\Pi_P^{\mathfrak{R}_0} = \left(\frac{\partial \mathfrak{R}_0}{\partial P} \right) \left(\frac{P}{\mathfrak{R}_0} \right).
 \tag{56}$$

Sensitivity analysis of the basic reproduction number of Anthrax \mathfrak{R}_{0a} and Listeriosis \mathfrak{R}_{0l} to each of the parameter values was computed separately, since the basic reproduction number of the coinfection model is usually

$$\mathfrak{R}_0 = \max \{ \mathfrak{R}_{0a}, \mathfrak{R}_{0l} \}.
 \tag{57}$$

TABLE 1: Sensitivity indices of \mathfrak{R}_{0a} to each of the parameter values.

Parameter	Description	Sensitivity Index
Ω_h	Human recruitment rate	1.2164
Ω_v	Vector recruitment rate	0.2433
β_h	Human transmission rate	0.1216
β_v	Vector transmission rate	0.0243
α	Anthrax recovery rate	-0.0037
μ_h	Human natural death rate	-0.0122
μ_v	Vector natural death rate	-0.0061
ϕ	Anthrax related death rate	-0.0065
θ	Modification parameter	$3.42913 * 10^{-6}$

6.1. *Sensitivity Indices of \mathfrak{R}_{0a} .* In this section, we derive the sensitivity of \mathfrak{R}_{0a} , to each of the parameters. Table 1 shows the detailed sensitivity indices of the basic reproduction number of Anthrax (\mathfrak{R}_{0a}) to each of the parameter values. From the values in Table 1, it can be observed that the most sensitive parameters are human transmission rate, vector transmission rate, human recruitment rate, and vector recruitment rate. Since the basic reproduction number is less than one, increasing the human recruitment rate by 10% would increase the basic reproduction number of Anthrax by 12.164%. However, decreasing the human recruitment rate by 10% would decrease the basic reproduction number of Anthrax by 12.164%. Moreover, decreasing human and vector transmission rates by 10% would decrease the basic reproduction number of Anthrax by 1.216% and 0.243%, respectively. However, increasing human and vector transmission rates by 10% would increase the basic reproduction number of Anthrax by 1.216% and 0.243%, respectively. The sensitivity analysis determines the contribution of each parameter to the basic reproduction number. This is an improvement of the work done by authors in [2, 3].

6.2. *Sensitivity Indices of \mathfrak{R}_{0l} .* In this section, we derive the sensitivity of \mathfrak{R}_{0l} to each of the parameters. The detailed sensitivity indices of the basic reproduction number of Listeriosis (\mathfrak{R}_{0l}) to each of the parameter values are shown in Table 2. We observe from the values in Table 2 that the most sensitive parameters are bacteria ingestion rate, Listeriosis related death, human recruitment rate, and Listeriosis contribution to environment. Decreasing the human recruitment rate by 10% would cause a decrease in the basic reproduction number of Listeriosis by 0.201487%. However, increasing the human recruitment rate by 10% would cause an increase in the basic reproduction number of Listeriosis by 0.201487%. Moreover, decreasing Listeriosis contribution to environment and bacteria ingestion rate by 10% would cause a decrease in the basic reproduction number of Listeriosis. Increasing Listeriosis contribution to environment and bacteria ingestion rate by 10% would cause an increase in the basic reproduction number of Listeriosis.

7. Numerical Methods and Results

In this section, we carried out the numerical simulations of the coinfection model to illustrate the results of the qualitative

analysis of the model which has already been performed. The variable and parameter values in Table 3 were used in the simulation of the coinfection model in (3). For the purposes of illustrations, we assumed some of the parameter values. Table 3 shows the detailed description of parameters and values that were used in the simulations of model (3). We used a Range-Kutta fourth-order scheme in the numerical solutions of the system of differential equations in model (3) by using matlab program.

7.1. *Simulation of Model Showing the Effects of Increasing Force of Infection on Infectious Anthrax and Listeriosis Populations Only.* In this section, we simulate the system of differential equations in model (3) by varying the human contact rate to see its effects on infected Anthrax population, infected Listeriosis population, and Anthrax-Listeriosis coinfecting population. This was done by setting the values of human contact rate as $\beta_h = 0.01, \beta_h = 0.02, \beta_h = 0.03$, and $\beta_h = 0.04$. Figure 3 shows an increase in the infected Anthrax population as the value of contact rate increases. Moreover, as the value of the human contact rate decreases, the number of Anthrax infected population decreases with time. However, an increase or decrease in the human contact rate increases or decreases the Listeriosis infected population with time as confirmed in Figure 4. The number of Anthrax-Listeriosis coinfecting population shows a sharp reduction in the number of individuals infected with both diseases but there is an increase in the number of infectious population as shown in Figure 5. An increase or decrease in the human contact rate shows an increase or decrease in the number of Anthrax-Listeriosis coinfecting population as indicated in Figure 5. Analysis of force of infection gives a better understanding of the effects of the contact rate which was not considered by the work of authors in [2, 3, 20].

7.2. *Simulation of Model Showing Infected Anthrax, Listeriosis, and Coinfecting Populations.* In this section, we simulate the model (3) to see the behaviour of Anthrax infected population, Listeriosis infected population, and Anthrax-Listeriosis coinfecting population. Figure 6 shows an increase in the number of Anthrax infected individuals and a sharp increase in the number of Listeriosis infected individuals. Figure 7 shows a sharp reduction in the number of Anthrax-Listeriosis coinfecting population from the beginning and it increases steadily at a point in time. Since the number of susceptible human populations increases in the system with time, there are higher chances of individuals being infected with Anthrax, Listeriosis, and Anthrax-Listeriosis coinfection. This is because the concept of mass action was one of the assumptions that was incorporated in our model.

7.3. *Simulation of Model Showing Susceptible Human Bacteria Populations.* In this section, we simulate model (3), to observe the behaviour of the susceptible human population and how the bacteria (carcasses) growth behaves with time in the epidemics. Figure 8 shows an increase in both the susceptible and bacteria growth. An increase in the number of susceptible from the beginning confirms the increase in

TABLE 2: Sensitivity indices of \mathfrak{R}_{0l} to each of the parameter values.

Parameter	Description	Sensitivity Index
Ω_h	Human recruitment rate	0.0201487
σ	Co-infected human recovery rate	$-5.41441 * 10^{-6}$
μ_h	Human natural death rate	-0.00014638
η	Listeriosis death rate among co-infected	$-5.41441 * 10^{-6}$
θ	Modification parameter	$3.42913 * 10^{-6}$
ν	Bacteria ingestion rate	0.0000402975
ρ	Listeriosis contribution to environment	0.0000309981
K	Concentration of carcasses	$-2.01487 * 10^{-10}$
δ	Listeriosis recovery rate	-0.0000402218
μ_b	Carcasses mortality rate	-0.0080595
m	Listeriosis related death	-0.0000402218

TABLE 3: Variable and parameter values of the coinfection model.

Parameter	Description	Value	Reference
ϕ	Anthrax related death rate	0.2	(Health line, Dec., 2015)
m	Listeriosis related death rate	0.2	Adak et al., 2002.
q	Anthrax death rate among co-infected	0.04	assumed
η	Listeriosis death rate among co-infected	0.08	assumed
β_h	Human transmission rate	0.01	[23]
β_v	Vector transmission rate	0.05	assumed
k	Anthrax waning immunity	0.02	assumed
μ_v	Vector natural death rate	0.0004	[23]
Ω_h	Human recruitment rate	0.001	assumed
Ω_v	Vector recruitment rate	0.005	[23]
α	Anthrax recovery rate	0.33	[24]
δ	Listeriosis recovery rate	0.002	assumed
ψ	Anthrax-Listeriosis waning immunity	0.07	assumed
ρ	Listeriosis contribution to environment	0.65	assumed
σ	Co-infected recovery rate	0.005	assumed
μ_b	Bacteria death rate	0.0025	assumed
μ_h	Human natural death rate	0.2	[23]
ω	Listeriosis waning immunity	0.001	assumed
θ	Modification parameter	0.45	assumed
ϵ	Co-infected who recover from Anthrax only	0.025	assumed
K	Concentration of carcasses	10000	[20]
ν	Bacteria ingestion rate	0.5	[20]

the number of Anthrax infection and Listeriosis infection in Figure 6. The increase in the number of susceptible human populations could be attributed to our model being an open system.

8. Conclusion

In this paper, we analysed the transmission dynamics of Anthrax-Listeriosis coinfection model. The compartmental model was analysed qualitatively and quantitatively to

fully understand the transmission mechanism of Anthrax-Listeriosis coinfection. Our model revealed that the disease-free equilibrium of the Anthrax model only is locally stable when the basic reproduction number is less than one and a unique endemic equilibrium whenever the basic reproduction number is greater than one. The disease-free equilibrium of the Listeriosis model only is locally stable when the basic reproduction number is less than one and a unique endemic equilibrium whenever the basic reproduction number is greater than one. Our model analysis

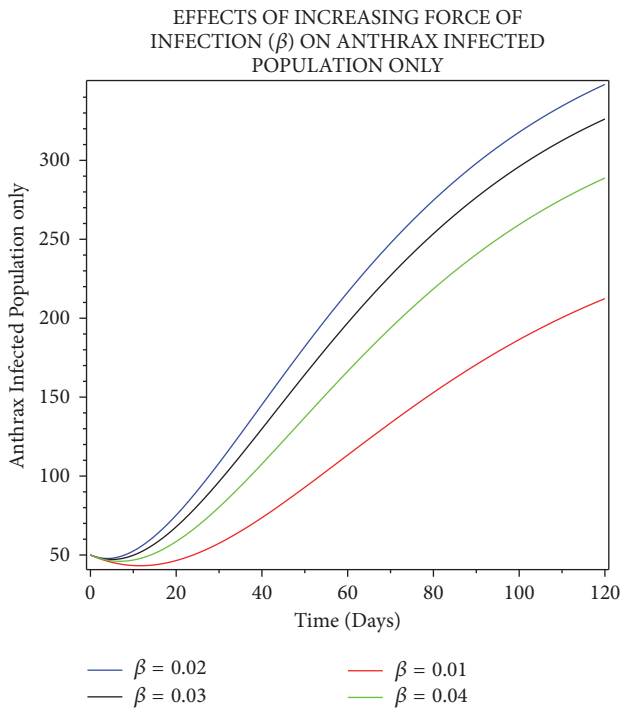


FIGURE 3: Simulation showing the effects of increasing the force of infection on Anthrax infected population only.

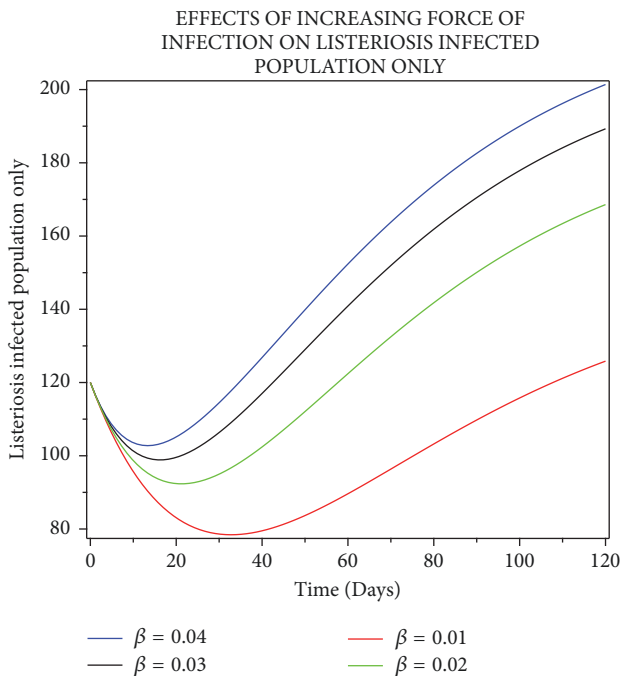


FIGURE 4: Simulation showing the effects of increasing the force of infection on Anthrax infected population only.

also reveals that the disease-free equilibrium of the Anthrax-Listeriosis coinfection model is locally stable whenever the basic reproduction number is less than one. The phenomenon of backward bifurcation was exhibited by our model. The biological implication is that the idea of the model been locally stable whenever the reproduction number is less than

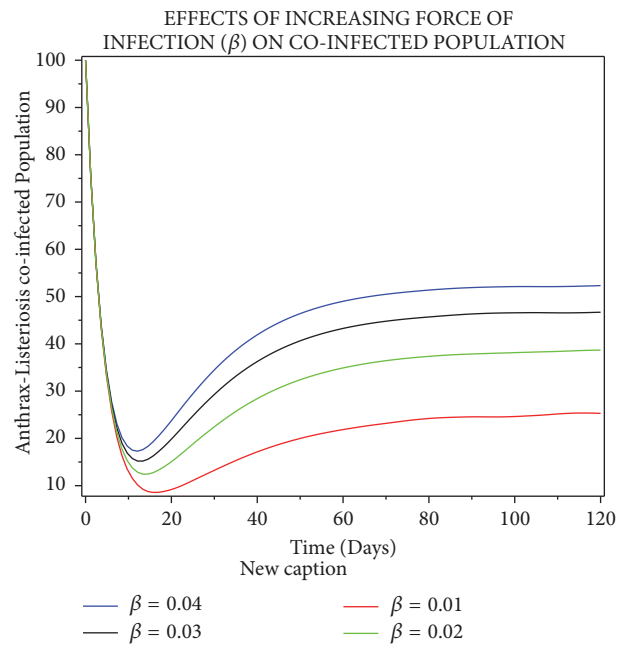


FIGURE 5: Simulation showing the effects of increasing the force of infection on Anthrax infected population only.

unity and unstable otherwise does not apply. This means that the Anthrax-Listeriosis coinfection model shows a case of coexistence of the disease-free equilibrium and the endemic equilibrium whenever the basic reproduction number is less than one.

We performed the sensitivity analysis of the basic reproductive number to each of the parameters to determine which parameter is more sensitive. The sensitivity indices of the basic reproduction number of Anthrax to each of the parameter values revealed that the most sensitive parameters are human transmission rate, vector transmission rate, human recruitment rate, and vector recruitment rate. Since the basic reproduction number is less than one, increasing the human recruitment rate would increase the basic reproduction number. This analysis is an improvement of the work done by [2, 3]. They considered the dynamics of Anthrax in animal population but never considered sensitivity analysis to determine the most sensitive parameter to the model.

The sensitivity indices of the basic reproduction number of Listeriosis to each of the parameter values shows that the most sensitive parameters are bacteria ingestion rate, Listeriosis related death, human recruitment rate, and Listeriosis contribution to environment.

We simulate the Anthrax-Listeriosis coinfection model by varying the human contact rate to see its effects on infected Anthrax population, infected Listeriosis population, and Anthrax-Listeriosis coinfecting population. This analysis is an improvement of the work done by authors in [2, 3, 20]. Our simulation shows an increase in the infected Anthrax population, an increase the number Listeriosis infected population, and an increase in the number of Anthrax-Listeriosis

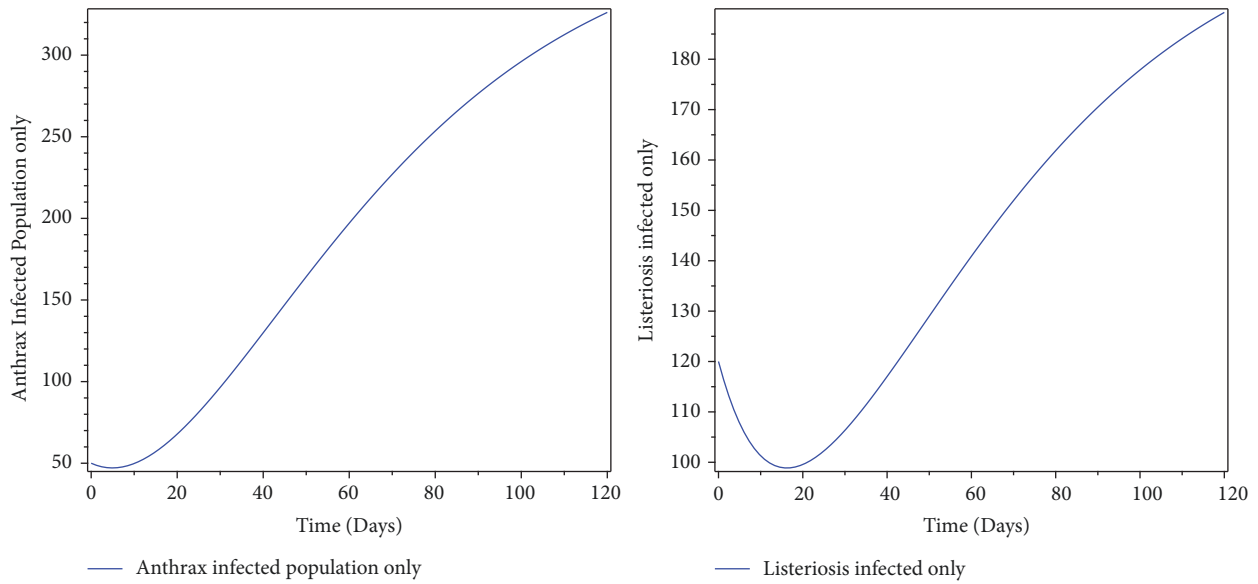


FIGURE 6: Simulation showing infected Anthrax and infected Listeriosis population.

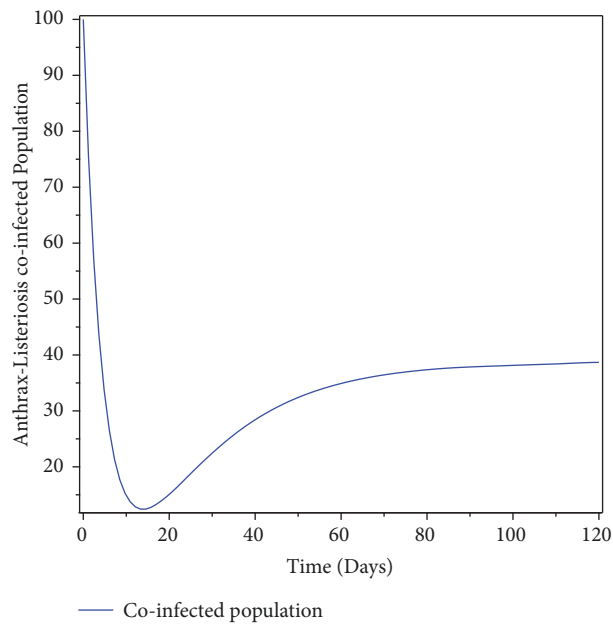


FIGURE 7: Simulation of model showing Anthrax-Listeriosis coinfection population.

coinfected population as the value of the human contact rate increases.

Data Availability

The data supporting this deterministic model are from previously published articles and they have been duly cited in this paper. Those parameter values taken from published

articles are cited in Table 3 of this paper. These published articles are also cited at relevant places within the text as references.

Conflicts of Interest

The authors declare that there are no conflicts of interest regarding the publication of this paper.

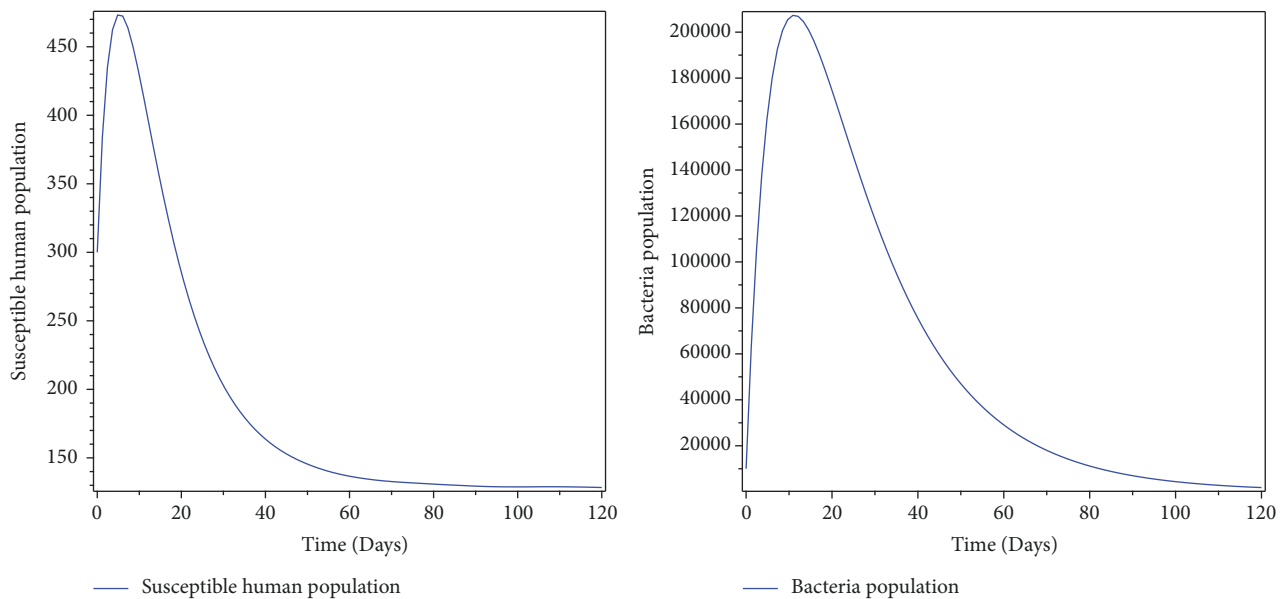


FIGURE 8: Simulation of model showing susceptible human and bacteria populations.

References

- [1] W. F. Schleich and D. Acheson, "Foodborne listeriosis," *Clinical Infectious Diseases*, vol. 31, no. 3, pp. 770–775, 2000.
- [2] C. M. Saad-Roy, P. van den Driessche, and A.-A. Yakubu, "A mathematical model of anthrax transmission in animal populations," *Bulletin of Mathematical Biology*, vol. 79, no. 2, pp. 303–324, 2017.
- [3] A. Friedman and A. A. Yakubu, "Anthrax epizootic and migration: persistence or extinction," *Mathematical Biosciences*, vol. 241, no. 1, pp. 137–144, 2013.
- [4] Z. Lu, X. Chi, and L. Chen, "The effect of constant and pulse vaccination on SIR epidemic model with horizontal and vertical transmission," *Mathematical and Computer Modelling*, vol. 36, no. 9–10, pp. 1039–1057, 2002.
- [5] A. A. Lashari and G. Zaman, "Optimal control of a vector borne disease with horizontal transmission," *Nonlinear Analysis: Real World Applications*, vol. 13, no. 1, pp. 203–212, 2012.
- [6] A. A. Lashari, "Optimal control of an SIR epidemic model with a saturated treatment," *Applied Mathematics & Information Sciences*, vol. 10, no. 1, pp. 185–191, 2016.
- [7] S. Mushayabasa and C. P. Bhunu, "Is HIV infection associated with an increased risk for cholera? Insights from a mathematical model," *BioSystems*, vol. 109, no. 2, pp. 203–213, 2012.
- [8] A. B. Gumel and S. M. Moghadas, "A qualitative study of a vaccination model with non-linear incidence," *Applied Mathematics and Computation*, vol. 143, no. 2–3, pp. 409–419, 2003.
- [9] T. K. Kar and A. Batabyal, "Stability analysis and optimal control of an SIR epidemic model with vaccination," *BioSystems*, vol. 104, no. 2–3, pp. 127–135, 2011.
- [10] O. D. Makinde, "Adomian decomposition approach to a SIR epidemic model with constant vaccination strategy," *Applied Mathematics and Computation*, vol. 184, no. 2, pp. 842–848, 2007.
- [11] T. T. Yusuf and F. Benyah, "Optimal control of vaccination and treatment for an SIR epidemiological model," *World Journal of Modelling and Simulation*, vol. 8, no. 3, pp. 194–204, 2012.
- [12] G. Zaman, Y. H. Kang, and I. H. Jung, "Optimal treatment of an SIR epidemic model with time delay," *BioSystems*, vol. 98, no. 1, pp. 43–50, 2009.
- [13] G. Zaman, Y. Han Kang, and I. H. Jung, "Stability analysis and optimal vaccination of an SIR epidemic model," *BioSystems*, vol. 93, no. 3, pp. 240–249, 2008.
- [14] O. Shaibu, D. M. Oluwole, and M. T. David, "Stability analysis and modelling of listeriosis dynamics in human and animal populations," *The Global Journal of Pure and Applied Mathematics (GJPAM)*, vol. 14, no. 1, pp. 115–137, 2018.
- [15] O. D. Makinde and K. O. Okosun, "Impact of chemo-therapy on optimal control of malaria disease with infected immigrants," *BioSystems*, vol. 104, no. 1, pp. 32–41, 2011.
- [16] K. Hattaf, M. Rachik, S. Saadi, Y. Tabit, and N. Yousfi, "Optimal control of tuberculosis with exogenous reinfection," *Applied Mathematical Sciences*, vol. 3, no. 5–8, pp. 231–240, 2009.
- [17] M. K. Borucki, J. Reynolds, C. C. Gay et al., "Dairy farm reservoir of *Listeria monocytogenes* sporadic and epidemic strains," *Journal of Food Protection*, vol. 67, no. 11, pp. 2496–2499, 2004.
- [18] H. W. Hethcote, "Qualitative analyses of communicable disease models," *Mathematical Biosciences*, vol. 28, no. 3–4, pp. 335–356, 1976.
- [19] N. C. Grassly and C. Fraser, "Mathematical models of infectious disease transmission," *Nature Reviews Microbiology*, vol. 6, no. 6, pp. 477–487, 2008.
- [20] K. O. Okosun and O. D. Makinde, "A co-infection model of malaria and cholera diseases with optimal control," *Mathematical Biosciences*, vol. 258, pp. 19–32, 2014.
- [21] P. van den Driessche and J. Watmough, "Reproduction numbers and sub-threshold endemic equilibria for compartmental models of disease transmission," *Mathematical Biosciences*, vol. 180, pp. 29–48, 2002.
- [22] C. Castillo-Chavez and B. Song, "Dynamical models of tuberculosis and their applications," *Mathematical Biosciences and Engineering*, vol. 1, no. 2, pp. 361–404, 2004.

- [23] S. Mushayabasa, T. Marijani, and M. Masocha, “Dynamical analysis and control strategies in modeling anthrax,” *Computational and Applied Mathematics*, vol. 36, no. 3, pp. 1333–1348, 2017.
- [24] R. Brookmeyer, E. Johnson, and R. Bollinger, “Modeling the optimum duration of antibiotic prophylaxis in an anthrax outbreak,” *Proceedings of the National Academy of Sciences of the United States of America*, vol. 100, no. 17, pp. 10129–10132, 2003.



Hindawi

Submit your manuscripts at
www.hindawi.com

